PHILOSOPHICAL TRANSACTIONS OF THE ROYAL SOCIETY A MATHEMATICAL, PHYSICAL & ENGINEERING SCIENCES

Respiratory dose of inhaled ultrafine particles in healthy adults

Chong S. Kim and Peter A. Jaques

Phil. Trans. R. Soc. Lond. A 2000 **358**, 2693-2705
doi: 10.1098/rsta.2000.0678

10.1098/rsta.2000.0678

Respiratory dose of inhaled ultrafine particles in healthy adults

By Chong S. Kim[1] and Peter A. Jaques[2]

[1]*Human Studies Division, National Health and Environmental Effects Research Laboratory, US Environmental Protection Agency, Research Triangle Park, NC 27711, USA* (kim.chong@epamail.epa.gov)

[2]*Center for Environmental Medicine and Lung Biology, University of North Carolina, Chapel Hill, NC 27599, USA*

Ultrafine particles (less than 0.10 μm in diameter) are ubiquitous in the atmosphere and possess unique physicochemical characteristics that may pose a potential health risk. To help elucidate the potential health risk, we measured respiratory dose of ultrafine particles (0.04, 0.06, 0.08 and 0.10 μm in diameter) in healthy young adults using a novel serial bolus-delivery method. Under normal breathing conditions (i.e. tidal volume of 500 ml and respiratory flow rate of 250 ml s^{-1}), bolus aerosols were delivered sequentially to a lung depth ranging from 50–500 ml in 50 ml increments and deposition was measured for each of ten equal-volume compartments.

Results show that regional deposition varies widely along the depth of the lung regardless of the particle sizes used. Peak deposition was found in the lung regions situated between 150 and 200 ml from the mouth. Sites of peak deposition shifted proximally with a decrease in particle size. Deposition dose per unit surface area was largest in the proximal lung regions and decreased rapidly with an increase in lung depth. Peak surface dose was 5–7 times greater than the average lung dose. The results indicate that local enhancement of dose occurs in normal lungs, and such a dose enhancement may play an important role in the potential health effects of ultrafine aerosols.

Keywords: ultrafine aerosol; regional lung deposition; respiratory dose; particulate matter; ambient aerosol

1. Introduction

Although the mass fraction of ultrafine particles in ambient particulate matter is small, their presence in great number and surface area has been a source of concern as a potential health hazard. In a recent epidemiological study, a decrement of lung function measured in asthmatic adults has been shown to correlate better with the number of ultrafine particles than with the mass of fine particles (Peters *et al.* 1997). Animal studies have shown that ultrafine particles were capable of causing acute toxic effects and even death after short-term exposure in rats and that the observed toxic effects were correlated better with the surface area than with the mass of particles (Oberdörster *et al.* 1992, 1995). However, most epidemiological studies consistently reported a good correlation between relative health risk and mass concentration of presumably fine particles (Schwartz 1994; Pope *et al.* 1995). At present, there is

Table 1. *Summary of subject characteristics and lung function test results*

(All values are mean ± SD of $n = 11$ each. FVC denotes forced vital capacity; FEV_1 denotes forced expired volume at 1 s; R_{aw} denotes airway resistance; FRC denotes functional residual capacity; TLC denotes total lung capacity.)

sex	age (yr)	height (cm)	FVC (ml)	FEV_1 (ml)	R_{aw} (cm H_2O l^{-1} s^{-1})	FRC (ml)	TLC (ml)
men	31 ± 4	173 ± 7	5388 ± 847	4404 ± 708	1.00 ± 0.6	3911 ± 892	6598 ± 980
women	31 ± 4	165 ± 6	4278 ± 587	3467 ± 540	1.24 ± 0.6	3314 ± 547	5282 ± 599

no clear explanation for how ambient particles can cause adverse health effects at low concentrations. As such, it is unclear whether there are differential roles for fine and ultrafine particles on health effects at ambient conditions. However, from the dosimetric point of view, a greater deposition dose poses a greater risk to health. Previous studies have shown that total lung deposition of ultrafine particles increases with a decrease in particle size, i.e. the smaller the particle size, the greater the lung deposition (Tu & Knutson 1984; Wilson *et al*. 1985; Schiller *et al*. 1986; Jaques & Kim 2000). Although the size-dependent deposition characteristics are different from those of fine and coarse particles for which lung deposition increases with an increase in particle size, total lung deposition values are generally comparable for ultrafine versus fine and coarse particles (Stahlhofen *et al*. 1989). However, inhaled particles deposit variably in different regions of the lung and this may result in a marked enhancement of dose in local regions, while overall lung dose may be considered to be safe. Because local regions receiving greater doses are likely to be affected more severely and may become initiating points for subsequent adverse health effects, assessment of local dose would be of great interest in evaluating potential health risk of inhaled particles. Previously, we have shown that local deposition dose can be many times greater than the average lung dose in healthy subjects for fine and coarse particles (Kim *et al*. 1996; Kim & Hu 1998). These results may not be applied directly to ultrafine particles because particles with different sizes deposit in the lung by different deposition mechanisms. Ultrafine particles deposit in the lung by diffusion, whereas fine and coarse particles deposit by gravitational sedimentation and inertial impaction. Therefore, it is important to know if there is any uniqueness in deposition patterns of ultrafine particles that can be related to detrimental health effects. In the present study, we measured total as well as detailed regional lung deposition for four different sizes of ultrafine particles under normal breathing conditions and compared the results with those obtained previously for fine and coarse particles. The purpose of the study was to obtain a detailed site–dose relationship for ultrafine particles in healthy lungs, which may be used for evaluating the potential health risk of ambient particulate matter.

2. Experimental methods

(*a*) *Subjects*

Twenty-two healthy adults (11 men and 11 women) ranging in age from 20 to 40 years old were studied. The subjects either had no history of smoking or had not smoked in the past five years. All subjects underwent a screening procedure that included

a complete medical history, physical examination, SMA-20 blood chemistry screen, and complete differential blood count. Those who passed the initial screening had their basic lung function measured by both spirometry and body plethysmography. Subject characteristics and lung function test results are shown in table 1.

(*b*) *Generation of ultrafine aerosols*

Ultrafine aerosols were generated by condensing sebacate oil (di-2-ethylhexyl sebacate) vapour on non-hygroscopic metallic nuclei particles. The aerosol generator consisted of a monodisperse condensation aerosol generator (model 3470, TSI Inc., St Paul, MN) and a nuclei aerosol generator using a nickel–chromium heating wire (80% Ni and 20% Cr and *ca.* 0.5 mm in diameter; Omega Engineering, Stamford, CT). The TSI aerosol generator uses NaCl aerosols as a source of condensation nuclei. However, ultrafine sebacate oil particles generated with NaCl nuclei were found to be somewhat hygroscopic. Therefore, NaCl nuclei were replaced with non-hygroscopic metallic nuclei. Briefly, metallic nuclei are produced by heating a coiled Ni–Cr wire (*ca.* 3–4 Ω) at low electric voltage (*ca.* 1.1–1.6 V AC). The nuclei aerosol (*ca.* 3 l min^{-1}) is then passed through a *boiler* in which sebacate oil is heated and vaporized at 70–100 °C. The mixture of nuclei and oil vapour from the boiler is passed through a *reheater* that is maintained at 190 °C and subsequently through an unheated vertical column designed to induce condensation of oil vapour on the surface of nuclei particles. The aerosols emerging from the generator are diluted with filtered air (*ca.* 100 l min^{-1}) and supplied to the inhalation system. In the present study, ultrafine aerosols with four different particle sizes were generated; 0.04, 0.06, 0.08 and 0.1 μm in number median diameter (NMD) with a geometric standard deviation (σ_g) in the range 1.27–1.34. The size distribution was measured using a scanning mobility particle sizer (SMPS) (model 3934, TSI Inc., St Paul, MN).

(i) *Inhalation system*

The core of the system consists of an ultrafine condensation particle counter (UCPC), an aerosol bolus-injection module, and an on-line data-acquisition system (see figure 1). In the bolus-injection module, test aerosols are introduced into the inspiratory line as a small bolus (half width of *ca.* 45 ml) by activating a solenoid valve. The duration of valve opening is initially set to 100 ms and adjusted to an appropriate value depending on flow and pressure conditions upstream. The aerosol chamber upstream of the solenoid valve is maintained at a positive pressure (1–5 cm H_20) slightly above room conditions to help inject the aerosol. During inhalation, the aerosol is sampled continuously into a UCPC (model 3025A, TSI Inc., St Paul, MN) at a rate of 25 ml s^{-1} via the sidearm port attached to the mouthpiece. In the UCPC, ultrafine particles pass through an alcohol vapour chamber (38 °C), and the mixture of the aerosol and vapour is introduced into a tube cooled to 4 °C in which alcohol vapour condenses on the surface of particles. As a result, ultrafine particles grow to a super-micrometre size, and the enlarged particles are detected by a laser sensor. The TSI UCPC outputs an aerosol signal averaged over a 2 s period. In the present system, the averaging circuitry was bypassed and aerosol signals were taken directly from the sensor for continuous output. Respiratory flow rates are measured by a pneumotachograph (Fleisch Size no. 1, Linton Instrumentation, Norfolk, UK) in conjunction with a pressure transducer (model 239, ±1.27 cm H_2O range,

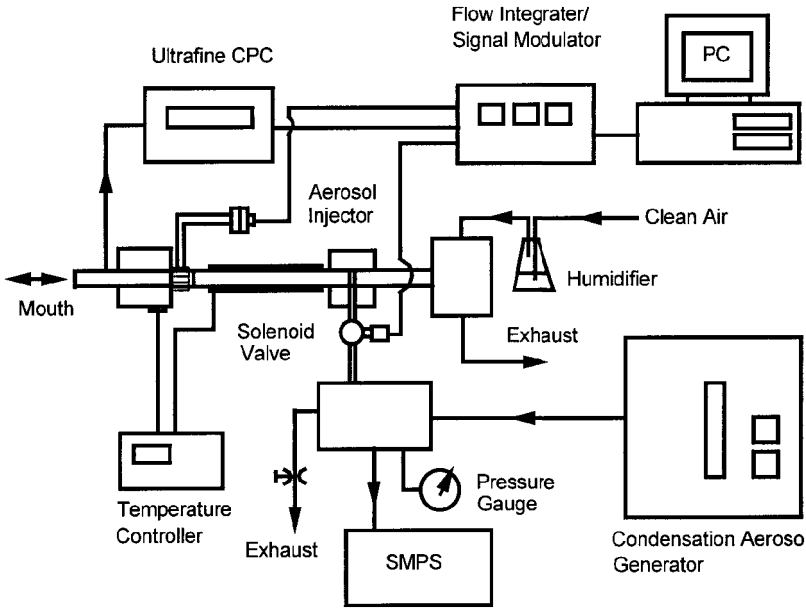

Figure 1. Experimental system used for determining regional lung deposition of ultrafine particles. CPC denotes condensation particle counter; PC, personal computer.

Setra Systems Inc., Acton, MA) that is connected to the mouthpiece in-line. Both flow and aerosol signals are supplied to an on-line data acquisition system at a rate of 200 Hz and subsequently analysed breath by breath.

(ii) *Bolus aerosol inhalation procedure*

In the serial bolus-delivery method, the subject first inhales clean air with a prescribed breathing pattern displayed on a computer screen. A small aerosol bolus (*ca.* 45 ml half-width) is then injected into the inspiratory air stream at a preselected time point while the subject continues to inhale a predetermined tidal volume and then exhales all the way to the residual volume. By changing injection time point, bolus aerosol can be delivered sequentially to different depths within the lung. The method has been described in detail elsewhere (Kim *et al.* 1996; Kim & Hu 1998). In the present study, the subjects inhaled bolus aerosols with a tidal volume (V_t) of 500 ml at a respiratory flow rate (Q) of 250 ml s^{-1}. A series of bolus aerosols was delivered sequentially to a lung penetration depth (V_p) ranging from 50–500 ml in 50 ml increments. In other words, the lung was divided into ten serial compartments, each with equal volume, and aerosol was delivered to one compartment at a time on each inhalation (see figure 2). During inhalation, aerosol concentration was monitored continuously by a UCPC. The peak concentration within the bolus was maintained at a UCPC output of between 6 and 8 V; 1 V was equivalent to approximately 100 000 particles cm^{-3}. For a given inhalation condition, at least five repeated measurements were obtained. The procedure was repeated for each of four different aerosols (d_p = 0.04, 0.06, 0.08 and 0.1 μm; d_p refers to number median diameter here and elsewhere). The total number of particles inhaled (N_{in}) and subsequently exhaled (N_{ex}) was calculated for each bolus inhalation, and the recovery

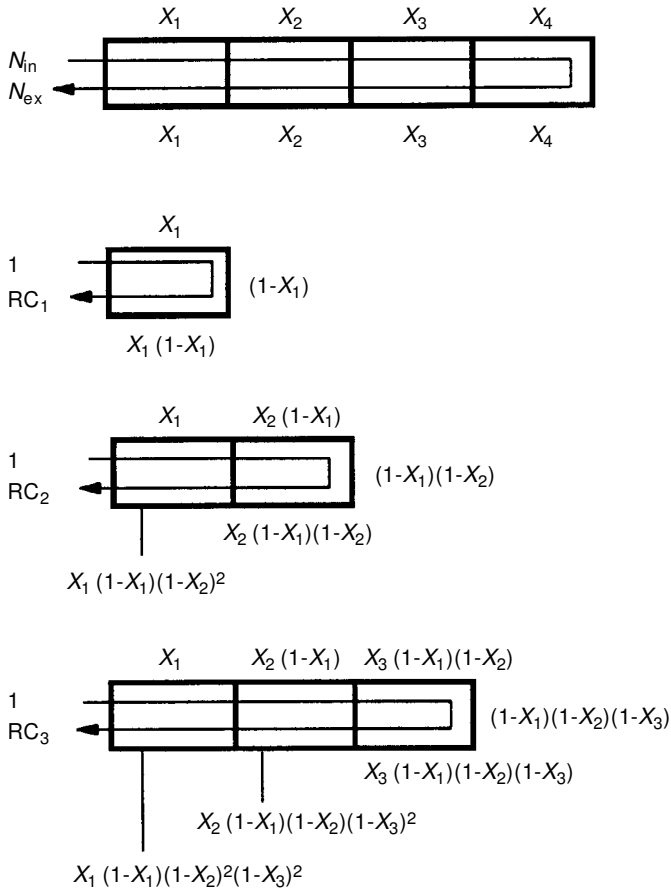

Figure 2. Calculation procedures for determining regional deposition efficiencies (X_i) and deposition fraction values for serial lung compartments. Bolus aerosol recovery (RC) is defined by the ratio of the total number of particles exhaled (N_{ex}) to the total number inhaled (N_{in}). Deposition efficiencies are assumed to be the same for inspiratory and expiratory flow in each compartment. Deposition fractions for inspiratory and expiratory phases are shown on the top and bottom of each compartment, respectively. Aerosol fractions remaining at end inspiration are as follows: $\mathrm{RC} = N_{ex}/N_{in}$; $\mathrm{RC}_1 = (1-X_1)^2$; $\mathrm{RC}_2 = (1-X_1)^2(1-X_2)^2$; $\mathrm{RC}_3 = (1-X_1)^2(1-X_2)^2(1-X_3)^2$; $\mathrm{RC}_n = \prod_{m=1}^{n}(1-X_m)^2$; $\mathrm{RC}_n/\mathrm{RC}_{n-1} = (1-X_n)^2$; $X_n = 1-\sqrt{(\mathrm{RC}_n/\mathrm{RC}_{n-1})}$.

($\mathrm{RC} = N_{ex}/N_{in}$) of bolus was obtained from each of ten volumetric compartments. Using a series of simultaneous mathematical formulae, local deposition efficiency (X) and subsequently local deposition fraction (LDF) were determined for each volumetric compartment (see figure 2). LDF was defined by the fraction of total aerosol inhaled that was deposited in each compartment.

3. Results and discussion

(*a*) *Deposition distribution in sequential volumetric lung regions*

The values of LDF of ultrafine aerosols ($d_p = 0.04$–0.1 μm) in sequential lung regions, each consisting of a 50 ml volume compartment, are shown in figure 3 for both men

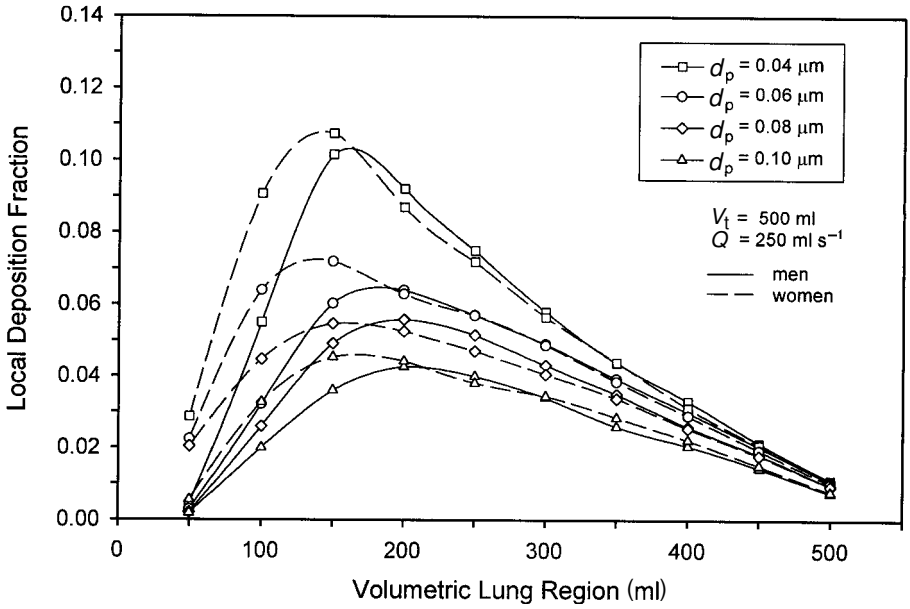

Figure 3. Regional deposition values in ten volumetric lung compartments for four different sizes of ultrafine particles for healthy men and women. The subjects inhaled the aerosols with a normal breathing condition: tidal volume of 500 ml and a breathing frequency of 15 breaths min^{-1}.

and women. All subjects inhaled ultrafine aerosols at a fixed breathing pattern consisting of a tidal volume of 500 ml and breathing frequency of 15 breaths min^{-1}. Mean respiratory flow rate was 250 ml s^{-1}. Figure 3 shows that LDF increases with V_p from the mouth, reaches the peak value, and then gradually decreases with a further increase in V_p. The deposition distribution pattern versus V_p was consistent regardless of particle size in both men and women. However, the peak height and position varied depending on particle size and gender of subjects. In men, the peak deposition was found in the lung region V_p = 150–200 ml for d_p = 0.1 μm. The peak position gradually shifted towards the mouth with decreasing particle size and was found in the lung region V_p = 100–150 ml for d_p = 0.04 μm. LDF was greater with smaller d_p throughout the entire lung regions. The increase in deposition was particularly prominent in the peak deposition regions. The peak deposition was nearly 2.5 times greater for d_p = 0.04 μm than for d_p = 0.1 μm. In women, deposition patterns were similar to those of men, but peak deposition regions shifted closer to the mouth and peak heights were slightly elevated for all d_p compared with those of men. LDF was consistently greater in shallow lung regions (V_p < 150 ml), particularly for regions of V_p = 0–50 ml and V_p = 50–100 ml. In deeper lung regions (i.e. V_p > 200 ml), deposition was comparable for men and women.

These results clearly show that regional deposition values vary widely in normal lungs and that local deposition dose can be many times greater than the average dose of the entire lung.

Peak deposition occurs in lung regions between 150 and 200 ml depth that encompasses the transition zone between the conducting airways and alveolar region. It should be noted that deposition efficiency in local lung regions increases monotonically with an increase in lung depth (Kim *et al.* 1996) because airway dimensions

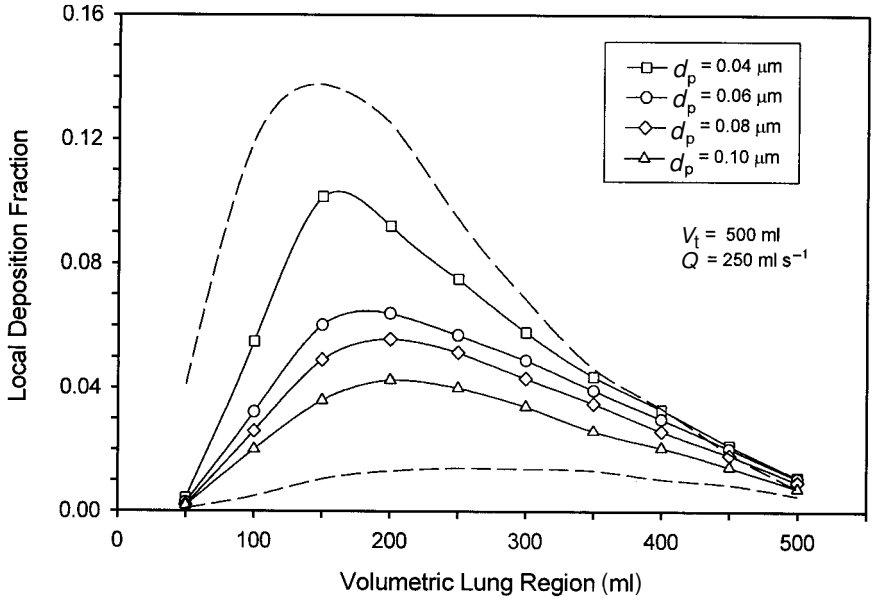

Figure 4. Regional deposition values of ultrafine particles compared with those of fine (1 μm) and coarse (5 μm) particles. Note that deposition values of ultrafine particles are confined between those of fine and coarse particles.

are smaller and particle residence time is longer in deeper lung regions. Therefore, deposition enhancement in the transition zone is not related to any unique structural features in the region, but is, rather, a logical outcome of a sequential filtration process in the respiratory airways. Deposition increases initially with an increase in lung depth and then decreases with a further increase in lung depth, because air reaching the deeper lung regions contains fewer particles. Longitudinal variation of lung deposition is an inevitable consequence of human lung anatomy and sequential respiratory airflow. Figure 3 shows that the longitudinal variation is more pronounced for smaller ultrafine particles (i.e. $d_p = 0.04\,\mu m$). This can be expected because the deposition efficiency of these small particles is very high (i.e. high diffusivity), resulting in a rapid increase in deposition in shallow lung regions followed by a rapid decrease in the deeper regions. Therefore, deposition tends to be concentrated over a small volumetric region of the lung. On the other hand, particles with low deposition efficiency (i.e. $d_p = 0.1\,\mu m$) can easily penetrate into deep lung regions, and deposition spreads out over a large area of the lung. The results also show that regional deposition is more pronounced in women than in men. Deposition enhancement is particularly noted in the proximal airway regions for women versus men. Similar findings have been reported previously for coarse particles (i.e. $d_p = 3$ and $5\,\mu m$; see Kim & Hu (1998)), and enhanced proximal deposition in women was attributed to small dimensions of the upper airways (i.e. pharynx and larynx), which, in turn, could result in an increase in inertial impaction. Inertial impaction is not relevant to deposition of ultrafine particles. However, airflow conditions in the upper airways are usually turbulent because of complex airway geometry, and enhanced turbulence in the smaller upper airways could result in an increase in diffusive deposition of ultrafine particles.

Table 2. *Three-compartment regional lung deposition values (%) for men and women*

(All values (mean ± SD) are percentage of total aerosol inhaled via the mouth. Breathing pattern was 500 ml tidal volume and 250 ml s^{-1} flow rate (i.e. 15 breaths per min).)

lung regions	particle diameter (μm)			
	0.04	0.06	0.08	0.10
men ($n = 11$)				
head	0.4 ± 0.7	0.3 ± 0.5	1.0 ± 1.9	0.2 ± 0.5
tracheobronchial	15.6 ± 4.6	9.2 ± 3.8	8.2 ± 3.7	5.7 ± 3.2
alveolar	33.1 ± 2.7	27.2 ± 3.8	23.9 ± 5.6	18.2 ± 6.2
total	49.2 ± 6.6	36.7 ± 7.2	33.1 ± 9.2	24.1 ± 8.9
women ($n = 11$)				
head	2.9 ± 2.5	2.2 ± 2.3	2.0 ± 2.2	0.6 ± 0.7
tracheobronchial	19.8 ± 3.4	13.6 ± 2.9	9.9 ± 2.7	7.8 ± 1.8
alveolar	32.2 ± 3.9	26.5 ± 4.1	22.7 ± 4.7	19.0 ± 2.9
total	54.9 ± 5.9	42.3 ± 6.9	34.7 ± 7.8	27.4 ± 4.1

In figure 4, deposition distributions of ultrafine particles for men are compared with those of fine and coarse particles that have been reported in earlier studies (Kim *et al*. 1996; Kim & Hu 1998). In the figure, it can be seen that deposition distributions of ultrafine particles are confined between those of fine ($d_p = 1$ μm) and coarse ($d_p = 5$ μm) particles, and that for particles of smaller size deposition patterns become more like those of coarse particles. In other words, very small ultrafine particles deposit in the lung more like large coarse particles. It should be noted that all of the present results are based on a typical breathing pattern (i.e. $V_t = 500$ ml and $Q = 250$ ml s^{-1}), and as such, the results may not be applied freely to different breathing conditions.

(*b*) *Three-compartment regional lung deposition*

Conventionally, regional lung deposition is expressed for three anatomic regions: head (larynx and above), tracheobronchial (TB) and alveolar region. Because these regions can be defined approximately by $V_p < 50$ ml for head, $V_p = 50$–150 ml for TB, and $V_p > 150$ ml for alveolar (Kim & Hu 1998), deposition in each of the regions can be obtained from the present sequential compartment results. For both men and women, deposition values in three regions are summarized in table 2 for a breathing pattern with $V_t = 500$ ml and $Q = 250$ ml s^{-1}. Total lung deposition values also are shown in table 2. All deposition values (mean ± SD) are a percentage of total aerosol inhaled via the mouth. Results show that deposition decreases consistently in all regions with an increase in particle size. This is consistent with the theory of particle deposition by diffusion: a greater deposition is expected with smaller ultrafine particles having greater diffusivity. Deposition in the head regions (mainly oropharynx and larynx) was very small (less than 3%). TB and alveolar deposition ranged from 5.7 to 15.6% and 18.2 to 33.1%, respectively, depending on particle size. Of the total deposition in the lung, 23–32% was deposited in TB and 68–77% was deposited in the alveolar region. These values are in general agreement with predictions by a

mathematical lung deposition model adopted by the International Commission on Radiological Protection (ICRP 1994) at a similar breathing condition. In table 1, it is noted that, compared with men, deposition in women is consistently greater in the TB region (21–47%), but was comparable or slightly smaller in the alveolar region. As a result, total lung deposition was greater in women than in men (5–15%). These results are consistent with those obtained by conventional non-bolus inhalation methods (Jaques & Kim 2000).

(*c*) *Surface dose in the regional lung compartment*

LDF values in sequential volume compartments of the lung are essential for deriving deposition values at specific anatomic regions, e.g. tracheobronchial versus alveolar region, as discussed above. However, such data are less useful for evaluating toxicological effects that may result from particle dose at a tissue level. Therefore, surface dose in each volumetric compartment was calculated and the result was plotted in figure 5 for the men's data. The surface dose was defined by LDF divided by surface area of each volumetric compartment. The surface area was calculated from Weibel's symmetric lung model at a lung volume of 3500 ml (Weibel (1963); see also table 3). The figure shows that surface dose is largest in the most proximal lung region and decreases rapidly with an increase in V_p. This was to be expected, because the surface area of the lung increases rapidly as the airways branch out into the deeper lung regions. Peak surface dose was 3–6 times (men; 5–7 times in women) greater than average lung dose, depending on particle size used.

Within each volumetric compartment, deposition distribution has been shown to be highly uneven, and a large portion (greater than *ca.* 80%) of deposition is focalized at specific anatomic sites, particularly in the conducting airway regions (Schlesinger *et al.* 1982; Kim & Fisher 1999). Therefore, a local tissue dose can be much greater than the peak surface dose shown in figure 5. Because adverse effects are likely to be initiated at the local site receiving greater tissue dose, this suggests that a risk assessment based on the average lung dose may substantially underestimate the potential health hazard of inhaled particles. The results also indicate that conducting airway regions take major insults of inhaled particles. This may be considered to be good because sensitive pulmonary regions may be protected from major insults of particles. However, the airway itself could be subject to serious injuries and may become a source of aetiology. This is particularly relevant to patients with obstructive airway disease, in whom particle deposition is greatly concentrated in the airway regions (Taplin *et al.* 1977; Kim & Kang 1997).

(*d*) *Exposure-dose considerations*

The deposition values presented above are based on a fraction of the total amount of aerosol inhaled and are independent of dose metrics. However, the actual practice of risk or toxicological assessment requires a specific dose metric, e.g. mass, number or surface area. Ultrafine particles contribute very little to mass concentrations of typical ambient aerosols, but they may constitute a large portion of the number and surface area of the aerosols (Whitby *et al.* 1974). To elucidate a potential role of ultrafine particles on adverse health effects, deposition dose needs to be analysed for appropriate dose metrics easily applicable to toxicological assessment. Table 3 shows the regional deposition dose of ultrafine particles ($d_p = 0.04\ \mu m$) in eight different

PHILOSOPHICAL TRANSACTIONS OF THE ROYAL SOCIETY A MATHEMATICAL, PHYSICAL & ENGINEERING SCIENCES

Table 3. *Regional deposition values of ultrafine particles* ($d_p = 0.04$ μm) *in sequential volumetric lung regions for men inhaling aerosols at a fixed concentration of* 10 μg m^{-3} *with a normal breathing pattern*[a]

(MDR denotes deposition rate of particle mass (density of particles equals 1 g cm^{-3}); NDR denotes deposition rate of particle number; S_pDR denotes deposition rate of particle surface area; and pS_pDR denotes deposition rate of projected surface area of particles.)

lung regions[b] (ml)	airway surface[c] (cm^2)	LDF	MDR (μg h^{-1})	NDR (particles h^{-1})	S_pDR (mm^2 h^{-1})	MDR/S (μg h^{-1} mm^{-2})	NDR/S (particles h^{-1} mm^{-2})	S_pDR/S (μm^2 h^{-1} mm^{-2})	pS_pDR/S (μm^2 h^{-1} mm^{-2})
50–100	927	0.055	0.247	7.37×10^9	37.0	2.66×10^{-6}	7.95×10^4	399.5	99.9
100–150	3 149	0.102	0.457	1.37×10^{10}	68.6	1.45×10^{-6}	4.34×10^4	217.8	54.5
150–200	4 540	0.090	0.406	1.21×10^{10}	61.0	8.95×10^{-7}	2.68×10^4	134.4	33.6
200–250	5 411	0.075	0.335	1.00×10^{10}	50.3	6.20×10^{-7}	1.85×10^4	93.0	23.3
250–350	11 953	0.101	0.453	1.35×10^{10}	68.0	3.79×10^{-7}	1.13×10^4	56.9	14.2
350–500	20 343	0.066	0.295	8.82×10^9	44.3	1.45×10^{-7}	4.34×10^3	21.8	5.5
50–150	4 076	0.156	0.703	2.10×10^{10}	105.5	1.73×10^{-6}	5.15×10^4	258.8	64.7
150–500	42 247	0.331	1.49	4.45×10^{10}	223.6	3.53×10^{-7}	1.04×10^4	52.9	13.2
50–500	46 323	0.487	2.19	6.55×10^{10}	329.3	4.73×10^{-7}	1.41×10^4	71.1	17.8

[a] Tidal volume of 500 ml and breathing frequency of 15 breaths min^{-1}.
[b] Lung regions between specified volumetric depths from the mouth.
[c] Airway surface area (S) calculated from Weibel's symmetric lung model at a lung volume of 3500 ml.

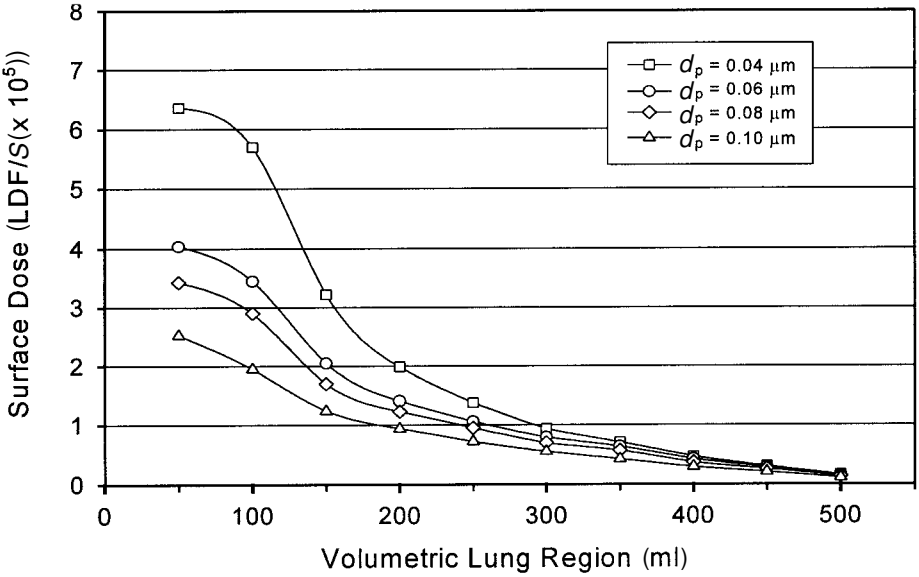

Figure 5. Surface dose of ultrafine particles in sequential lung-volume compartments. Surface dose is defined by LDF divided by the surface area (S in cm^2) of the same local compartment.

dose metrics for men inhaling the aerosol at a fixed concentration of 10 $\mu g\,m^{-3}$ with a normal breathing pattern at rest (i.e. $V_t = 500$ ml, $Q = 250\ ml\,s^{-1}$). The ambient concentration of 10 $\mu g\,m^{-3}$ is rarely expected for ultrafine particles, even in heavily polluted areas, but it was used as a reference concentration in the present calculation because, in epidemiological studies, the health risk of exposure to particulate pollutant has been routinely analysed for an increment of 10 $\mu g\,m^{-3}$ (Pope *et al.* 1995). In table 3, it can be seen that the whole lung dose of 0.04 μm particles may accumulate at a rate of 2 μg in mass, 6.6×10^{10} particles in number, and 329 mm^2 in surface area per hour under the exposure conditions described above (see bottom row). If these values are normalized by the surface area of the lung, the deposition rate will be 4.7×10^{-7} μg in mass, 1.4×10^4 particles in number, 71 μm^2 in surface area, and 18 μm^2 in projected surface area per hour in a 1 mm^2 area of the surface of the lung. Regional surface doses vary depending on values of local LDF and surface area, but it can be 5–6 times greater than the average surface dose (see the first row of table 3). These results are useful for estimating microscopic cellular or tissue doses if the number of specific cells or tissue volumes are known at the local lung regions. It should be noted that local particle burdens do not necessarily accumulate at the same rate as the deposition rate discussed above because particles are constantly cleared out of the deposition site by mucociliary or other transport mechanisms. Dose accumulation depends on the net balance between deposition and clearance. The results shown in table 3 did not consider clearance of particles, and, therefore, may be considered as a worst-case scenario for local dose accumulation. Although table 3 provides data for only one particle size, the data may be used as a guide for estimating deposition dose of particles of different sizes. LDF values of different ultrafine particles are shown in figure 3, and those of fine and coarse particles can be obtained from our earlier reports (Kim *et al.* 1996; Kim & Hu 1998).

4. Conclusions

Detailed regional deposition of ultrafine particles was measured in healthy men and women under normal breathing conditions at rest by a novel bolus-delivery method. From the results, the following conclusions can be drawn.

(1) Deposition of ultrafine particles in serial compartments of the lung varies widely along the volumetric depth of the lung. Peak deposition occurs in the transition zone between the conducting airways and alveolar region.

(2) Proximal airway regions receive the largest surface dose that amounts to a value several times greater than the average lung dose.

(3) Women receive a greater dose than men in the head and tracheobronchial regions.

Because adverse health effects are more likely to develop from local sites that are subject to excessive particle dose, the present results for local peak dose and dose distribution may prove to be useful for understanding the potential health risk of exposure to ultrafine particles.

Disclaimer

Although the research described in this article has been supported by the United States Environmental Protection Agency, it has not been subjected to Agency review and therefore does not necessarily reflect the views of the Agency and no official endorsement should be inferred. Mention of trade names or commercial products does not constitute endorsement or recommendation for use.

The authors thank Paulette DeWitt of the US EPA for skilful performance of pulmonary function tests on volunteer subjects, and the medical staff of the US EPA Human Studies Facility for a careful screening of study subjects.

References

ICRP (International Commission on Radiological Protection) 1994 Human respiratory tract model for radiological protection. *Ann. ICRP* **66**, 50, 423.

Jaques, P. A. & Kim, C. S. 2000 Measurement of total lung deposition of inhaled ultrafine particles in healthy men and women. *Inhal. Toxicol.* **12**, 715–731.

Kim, C. S. & Fisher, D. M. 1999 Deposition characteristics of aerosol particles in sequentially bifurcating airway models. *Aerosol Sci. Technol.* **31**, 198–220.

Kim, C. S. & Hu, S. C. 1998 Regional deposition of inhaled particles in human lungs: comparison between men and women. *J. Appl. Physiol.* **84**, 1834–1844.

Kim, C. S. & Kang, T. C. 1997 Comparative measurement of lung deposition of inhaled fine particles in normal subjects and patients with obstructive airway disease. *Am. J. Respir. Crit Care Med.* **155**, 899–905.

Kim, C. S., Hu, S. C., DeWitt, P. & Gerrity, T. R. 1996 Assessment of regional deposition of inhaled particles in human lungs by serial bolus delivery method. *J. Appl. Physiol.* **81**, 2203–2213.

Oberdörster, G., Ferin, J., Gelein, R., Sonderholm, S. C. & Finkelstein, J. 1992 Role of the alveolar macrophage during lung injury: studies with ultrafine particles. *Environ. Health Perspect.* **97**, 193–199.

Oberdörster, G., Gelein, R. M., Ferin, J. & Weiss, B. 1995 Association of particulate air pollution and acute mortality: involvement of ultrafine particles? *Inhal. Toxicol.* **7**, 111–124.

Peters, A., Wichmann, H. E., Tuch, T., Heinrich, J. & Heyder, J. 1997 Respiratory effects are associated with the number of ultrafine particles. *Am. J. Respir. Crit. Care Med.* **155**, 1376–1383.

Pope, C. A., Dockery D. W. & Schwartz, J. 1995 Review of epidemiological evidence of health effects of particulate air pollution. *Inhal. Toxicol.* **7**, 1–18.

Schiller, C. F., Gebhart, J., Heyder, J., Rudolf, G. & Stahlhofen, W. 1986 Factors influencing total deposition of ultrafine aerosol particles in the human respiratory tract. *J. Aerosol Sci.* **17**, 328–332.

Schlesinger, R. B., Gurman, J. L. & Lippmann, M. 1982 Particle deposition within bronchial airways: comparison using constant and cyclic inspiratory flows. *Ann. Occup. Hyg.* **26**, 47–64.

Schwartz, J. 1994 Air pollution and daily mortality: a review and meta-analysis. *Environ. Res.* **64**, 36–52.

Stahlhofen, W., Rudolf, G. & James, A. C. 1989 Intercomparison of experimental regional aerosol deposition data. *J. Aerosol Med.* **2**, 285–308.

Taplin, G. W., Tashkin, D. P., Chopra, S. K., Anselmi, O. E., Elam, D., Calvarese, B., Coulson, A., Detels, R. & Rokaw, S. N. 1977 Early detection of chronic obstructive pulmonary disease using radionuclide lung imaging procedures. *Chest* **71**, 567–575.

Tu, K. W. & Knutson, E. O. 1984 Total deposition of ultrafine hydrophobic and hygroscopic aerosols in the human respiratory system. *Aerosol Sci. Technol.* **3**, 453–465.

Weibel, E. R. 1963 *Morphometry of the human lung*. Academic.

Whitby, K. T., Clark, W. E., Marple, V. A., Sverdrup, G. M., Sem, G. J., Willeke, K., Liu, B. Y. H. & Pui, D. Y. H. 1974 Characterization of California aerosols. I. Size distribution of freeway aerosol. *Atmos. Environ.* **9**, 463–482.

Wilson Jr, F. J., Hiller, H. C., Wilson, J. D. & Bone, R. C. 1985 Quantitative deposition of ultrafine stable particles in the human respiratory tract. *J. Appl. Physiol.* **58**, 223–229.